Journal Pre-proof

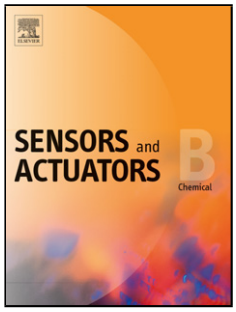

Aluminum-based self-powered hyper-fast miniaturized sensor for breath humidity detection

Marko V Bošković (Conceptualization) (Validation) (Investigation) (Writing - review and editing), Milija Sarajlić (Conceptualization) (Validation) (Investigation) (Writing - original draft) (Supervision), Miloš Frantlović (Investigation) (Writing - review and editing), Milče M Smiljanić (Investigation) (Writing - review and editing), Danijela V Randjelović (Investigation) (Writing - review and editing), Katarina Cvetanović Zobenica (Investigation) (Writing - review and editing), Dana Vasiljević Radović (Investigation) (Writing - review and editing) (Project administration) (Funding acquisition)

PII: S0925-4005(20)30981-3

DOI: https://doi.org/10.1016/j.snb.2020.128635

Reference: SNB 128635

To appear in: *Sensors and Actuators: B. Chemical*

Received Date: 23 March 2020

Revised Date: 7 July 2020

Accepted Date: 22 July 2020

Please cite this article as: Bošković MV, Sarajlić M, Frantlović M, Smiljanić MM, Randjelović DV, Zobenica KC, Radović DV, Aluminum-based self-powered hyper-fast miniaturized sensor for breath humidity detection, *Sensors and Actuators: B. Chemical* (2020), doi: https://doi.org/10.1016/j.snb.2020.128635

Aluminum-based self-powered hyper-fast miniaturized sensor for breath humidity detection

Marko V Bošković, Milija Sarajlić*, Miloš Frantlović, Milče M Smiljanić, Danijela V Randjelović, Katarina Cvetanović Zobenica, Dana Vasiljević Radović

University of Belgrade, Institute of Chemistry, Technology and Metallurgy, Center of Microelectronic Technologies (ICTM CMT), Njegoševa 12, 11000 Belgrade, Serbia

*Corresponding author: milijas@nanosys.ihtm.bg.ac.rs

Graphical abstract

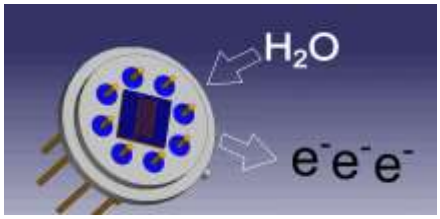

Highlights:

- Self-powered sensor provides a solution for battery-free operation
- Chemical energy harvesting at the basis of breath detection
- Extremely rapid response to high humidity levels

Abstract

An aluminum-based, self-powered, miniaturized sensor for breath humidity detection is presented. The sensor is designed as an interdigitated capacitor made out of sputtered aluminum 1% silicon (Al 1%Si) thin film, 700 nm thickness, with digits 1.5 mm long, 0.01 mm wide and 0.01 mm clearance between them. The voltage on the open end of the sensor is generated when the surface is covered with a thin layer of water vapor, for instance if a person blows on it. The voltage generated is up to 1.5 V. The voltage generation is based on an electrochemical process of interaction between aluminum, water and oxygen from air, similar to the operation of an aluminum-air battery. The rise time of the signal during water vapor (or breath) detection is as small as 10 ms which makes it one of the fastest humidity sensors reported to date. The relaxation time is in the range of 50 ms. To make detection possible, the sensor surface needs to be activated by native oxide removal with the help of

electric current and de-mineralized water droplet. Usability of the sensor was demonstrated in the detection of human breathing, where the sensor managed to follow the cycles of inhaling and exhaling.

Keywords: self-powered; breath detection; humidity; miniaturized sensor; aluminum-air battery; chemical energy harvesting.

1. Introduction

Breath detection is used in medical monitoring of the patient condition [1, 2, 3]. Breath detection can be achieved by monitoring relative humidity (RH) of the exhaled air since RH in this case is higher than 95 % [4, 5, 6, 7, 8, 9]. Key characteristics of the sensors suitable for breath humidity detection are: sensitivity to RH above 90%, response speed, repeatability, longevity, power consumption, size of the sensor, toxicity and volatility of the construction materials.

There is a huge number of different techniques and sensors for RH measurements in air. Most of the books or review articles on the subject cover only limited number of different techniques [10, 11, 12, 13]. In this introduction the accent is on humidity sensors for breath detection applications, self-powered sensors and miniaturized sensors.

Humidity sensors vary widely in construction and principle of operation. Bi et al. show ultrahigh sensitivity of graphene oxide to humidity [14]. The authors claim that the sensor has up to 10 times higher sensitivity than other capacitive humidity sensors to date (2013). Borini et al. show ultrafast graphene oxide (GO) humidity sensor which can react to a person whistling in around 30 ms [15]. This sensor has a structure of an interdigitated capacitor, with electrodes made out of Ag on a polyethylene naphthalate (PET) substrate and sprayed GO sensing element.

Many humidity sensors have the structure of an interdigitated capacitor. These structures are typically used with standard electrochemical techniques such as Square Wave Voltammetry or Impedance Spectroscopy [16, 17]. Cai et al. have made an all-graphene humidity sensor in the shape of an interdigitated capacitor, produced by laser direct writing [18]. The sensor is read out by a smartphone app where the input signal is a rectangular voltage wave.

The class of potentiometric sensors represents the sensors which are producing electromotive force (EMF) i.e. voltage on the open end of the sensor during detection of the target substance [19, 20, 21, 22, 23, 24]. Potentiometric sensors could be miniaturized or made as wearable sensors. Choi et al. developed a potentiometric wearable sensor for sweat chloride biomarker measurements [25]. In the field of humidity measurements there are only few realizations with potentiometric sensors. One attempt was given in 1995 by Toshikatsu Sata [26] where the author tested the strips 30 mm x 5 mm, cut from a composite membrane. On 100% RH the system responded with 350 mV EMF. There have been also other attempts but with a limited success [27, 28].

Another type of chemical sensors whose principle of operation is based on energy generation in the process of sensing are fuel cell sensors. Zhang et al. fabricated a fuel cell sensor based on GO which is especially selective towards ethanol and can be used as an alcohol test [29].

This sensor produces the current up to 5 μA and it takes at least 20 s before it reaches the maximum output. Ghavidel et al. fabricated fuel cell-based sensor for breath alcohol detection with electrodes made of Pt-Mn/C and Pt-Cu/C alloy [30]. In this way significantly less Pt is used for the purpose of alcohol detection. It is difficult to make a miniaturized fuel cell based sensor because the fuel cell construction is rather complicated [31].

In recent years, self-powered sensors are getting a lot of attention [32, 33, 34]. The term "self-powered" refers to a sensor which is having a power supply harvesting the energy related to the measurement. Zhang et al. made a respiration sensor based on energy harvesting from abdomen movements [35]. Wen et al. harvested the energy from the breath blow power and performed the alcohol test simultaneously [36]. Cui et al. manufactured an ammonia nanosensor powered by triboelectric nanogenerator (TENG) [37].

There are only few developments where a self-powered sensor does not require built-in energy harvesting device, but it is producing energy by itself through the sensing process. An interesting development in this sense was made recently (2018, 2019) by the group of researchers, Shen et al. [38, 39] and Xiao et al. [40]. The authors fabricated nano-fiber structure made of TiO_2 which forms a sponge-like device capable of producing electricity in the contact with water vapor. They showed that this structure is capable of functioning as a humidity sensor and the breath detector. The rise time of the signal was in the range of 2-3 s and the fall time was in the range of 6-7 s. The voltage generated during the water vapor sensing was up to 500 mV. Previously, a similar concept was used by another group of authors, for humidity detection based on GO thin film [41, 42]. In these developments a humidity sensor was capable of producing electricity in the process of sensing water vapor itself [38 - 44]. This would be the true-self-powered chemical sensor.

In this work, the sensor for breath humidity detection is presented. The sensor produces necessary energy in the process of measurement, i.e. during water vapor detection. No additional power source is needed for the detection of water vapor to occur. It is made in the form of an interdigitated capacitor with the digits made out of sputtered aluminum 1% silicon (Al 1%Si), 1.5 mm long and 10 μm wide with 10 μm clearance between them. The structure is fabricated by direct laser writing in vector mode and subsequent wet etching. The voltage at the open end of the sensor is generated when a layer of water vapor covers the surface of Al 1%Si thus making a reaction between aluminum and water which in turn generates electrons. This process is already known in the operation of aluminum-air battery [45, 46, 47]. The voltage generated is up to 1.5 V. The sensor is very fast with the rise time of the signal down to 10 ms and the relaxation time of about 50 ms. There are only few sensors reported to date which have the reaction time (or rise time) shorter than 100 ms [5, 15]. In this sense the sensor presented here comes into the class of the fastest humidity sensors reported to date. The sensor practicality has been demonstrated by applying it to human breath detection.

2. Material and methods

2.1 Fabrication

The sensor is fabricated on a silicon wafer, 3" diameter, 380 μm thickness, <100> orientation, 3.5 Ωcm resistivity, n-type, single side polished. Thermal oxidation of the wafer was done at 1150^{0}C for 70 min resulting in 0.6 μm thick oxide formed on both sides. The thin film sputtering process was tried with pure aluminum target and aluminum 1% silicon (Al 1%Si) target. It was obvious by optical inspection that Al 1%Si has less surface oxide after sputtering. For this reason Al 1%Si was chosen to be used in this experiment. On top of the thermally grown SiO_2, on the polished side of the wafer, a layer of Al 1%Si was deposited by DC magnetron sputtering. The thickness of Al 1%Si layer was 0.7 μm as verified by stylus profilometry (Talystep, Taylor Hobson, UK). For the particular application which was planned here, it is favorable that the layer of Al 1%Si is relatively thick because this material is consumed in the process of sensor operation. On the other hand, the thickness should be relatively small in order to enable better control of the line width in the process of chip fabrication. The chosen thickness was a good compromise between these two requests.

Fig. 1 The illustration of one part of the fabrication procedure, **a)** Direct laser writing, **b)** Zoom into the interdigitated structure, **c)** The illustration of the finished chip mounted on the TO-8 housing. The digits are enlarged in order to show the concept of the sensor.

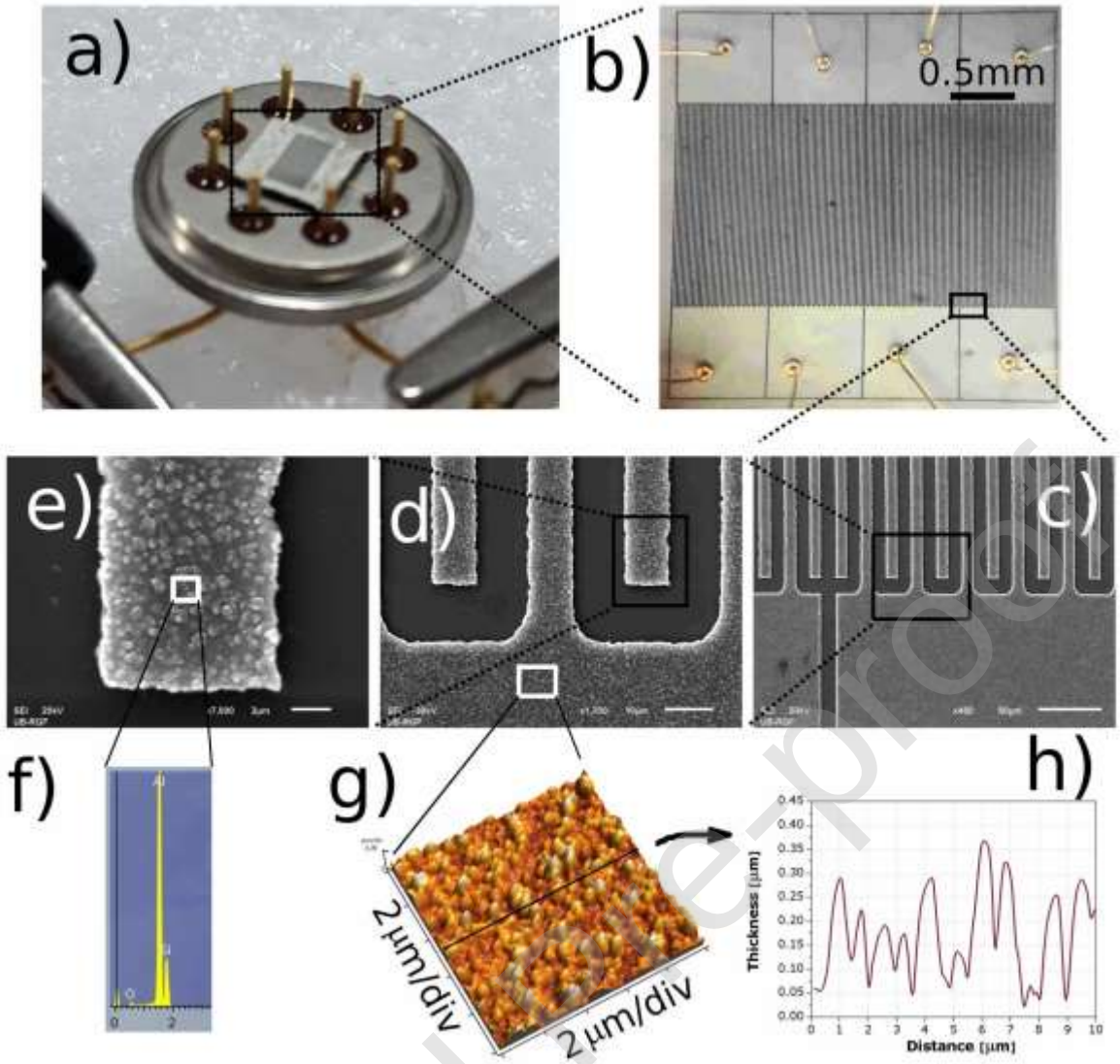

Fig. 2 a) Finished sensor mounted on TO-8 housing, **b)** The surface of the wire bonded sensor as seen on stereo microscope, c) Scanning electron microscope (SEM) image of the zoomed region, scale bar 50 µm, **d)** SEM image, scale bar 10 µm, **e)** SEM image, scale bar 2 µm, **f)** material analysis as done by SEM mass spectrometer, Oxygen 11%, Aluminum 62%, Silicon 27%, **g)** Atomic Force Microscope (AFM) image of the surface specimen, **h)** The profile of AFM measured surface along the characteristic line.

On top of Al 1%Si layer, 0.5 µm thick layer of photoresist (MicroChemicals, Germany) was deposited by spin coating. Direct laser writing in vector mode was performed using the Laser Writer (LW405, MicroTech, Italy). Subsequent wet etching in the solution 80 ml H_3PO_4, 5 ml HNO_3, 5 ml CH_3COOH, 10 ml H_2O, has formed the structure of interdigitated capacitor build out of Al 1%Si thin film, Fig. 1. In the wafer, the matrix of 4x4 chips was made. The wafer was diced and all 16 chips were glued by thermally and electrically isolating epoxy to the TO-8 housing, Fig. 1. Wire bonding with gold wire, 18 µm in diameter was done from the sensor pads to the housing pins. Optical microscopy, SEM and AFM images of the finished sensor are given in Fig. 2. The single sensor chip contains four separate batteries which are independently connected to the housing pins, Fig. 2 b). Active surface of a single battery is 1.58 mm x 0.74 mm or 1.17 mm^2.

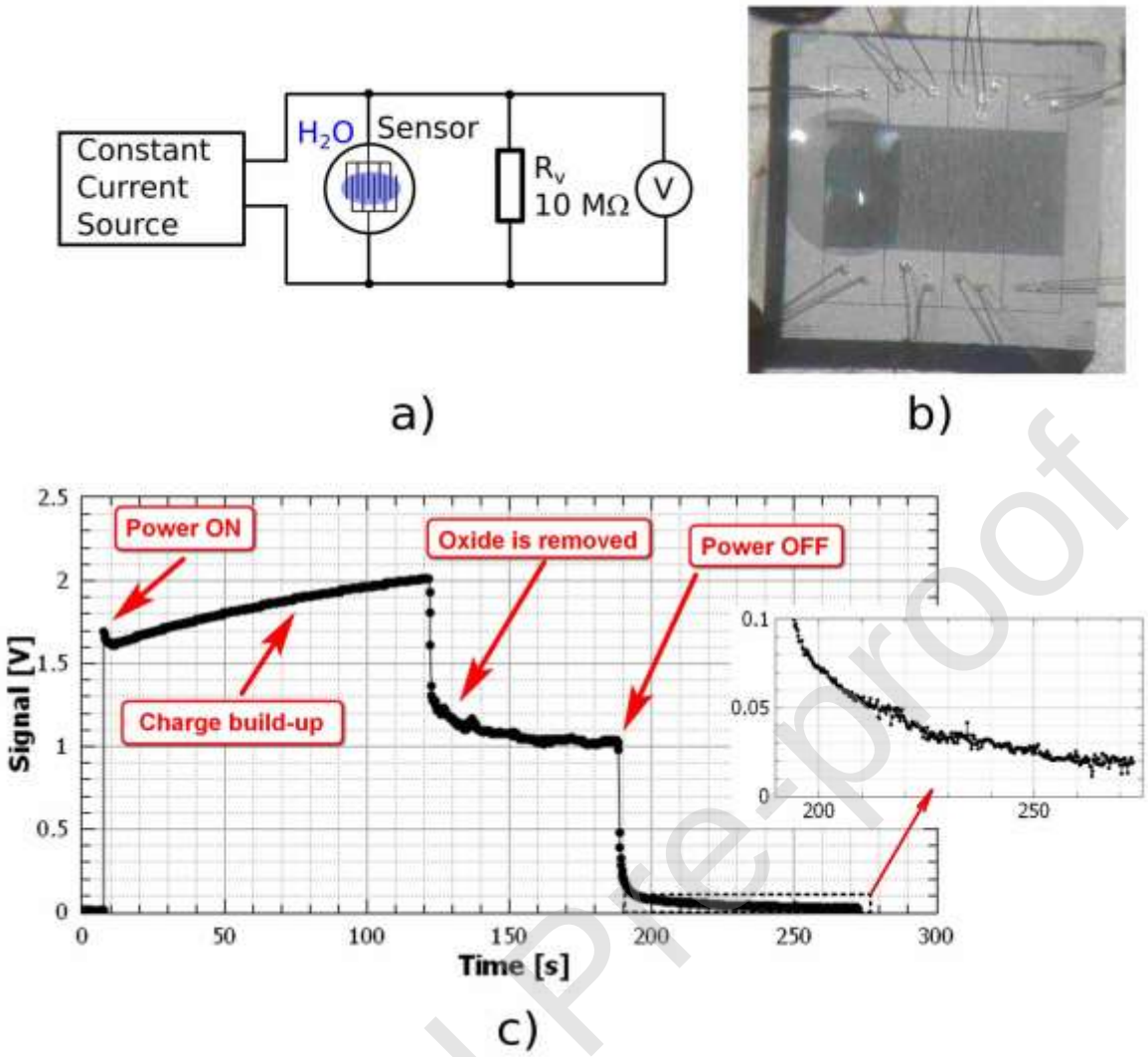

Fig. 3 a) Schematic of the activation set up. **b)** The micrograph of the sensor with a droplet of water on the surface as pictured on a stereo microscope. **c)** Diagram of the activation process.

2.2 Surface activation

After fabrication, the sensor is not active, i.e. it gives no output during interaction between the surface and the water vapor. This is probably a consequence of the surface oxide present on the sensor digits which was built-up during the sputtering process. The electrode activation is a common process in electrochemistry [48].

In order to activate the surface, a droplet of de-mineralized (DM) water was placed on top of the sensor's digits and the constant current of 0.5 μA was applied from the Constant Current Source (Keithley 220, Programmable Current Source), Fig. 3. The voltage at the sensor's electrical connection was monitored by the voltmeter (Keysight 34461A Multimeter) Fig. 3. The input resistance of the voltmeter was 10 MΩ. There are three distinct parts of the cleaning process. In the first part, Fig. 3 c), the voltage output of the sensor was increasing in the form which resembles the

charging of an electrolytic capacitor. It is believed that in this part the sensor is behaving as an electrolytic capacitor with the sensor digits as metal electrodes, DM water as electrolyte and surface oxide on the sensor digits as insulator. After certain period of charging of the electrolytic capacitor, a sudden drop in the voltage was observed. It is believed that this drop corresponds to the surface oxide removal. The same procedure was performed on all fabricated chips and on each battery in the chips and this characteristic behavior was always present. After this point the sensor is active in the sense it would react to the water vapor on its surface and produce electricity. The power from the current source was subsequently turned off and the voltage output of the sensor went exponentially to zero. This behavior is magnified in inset of Fig. 3 c). The activation procedure was necessary to be performed only once for each battery and after that the sensor is ready for use as a breath humidity detector.

3. Results and Discussion

3.1 Water vapor test

In order to test the sensor response to 100% humidity, the experiment with the source of water vapor was performed, Fig. 4. The thermally isolated glass cup was filled with hot water, 95^{o}C temperature, and brought underneath the sensor at the distance of 3-4 cm below the sensor`s surface. The sensor was turned upside down so that the active surface is facing the source of water vapor Fig. 4 a,b). In this way, the sensor is exposed to 100% RH which produces the signal (voltage) at the open end of the sensor. The humidity level, to which the sensor was exposed, has risen instantaneously from RH in the lab (around 50%) to RH of 100%. The glass cup was held underneath the sensor for a second or so, then it was swiftly removed in order to produce a short flush of water vapor on the sensor surface. The water vapor flush was deliberately of random intensity and the amount of vapor coming to the sensor surface was not controlled. The sensor was connected to a voltmeter (Keysight 34461A Multimeter). Input resistance of the voltmeter was 10 MΩ. The cables from the sensor to the voltmeter were shielded and the shield was grounded. The voltmeter was also grounded. This was necessary in order to prevent interference of external electromagnetic fields, and to reduce the noise in the system. The sensor was probed in this way in the time span of 38 days. The test was performed once per day, mainly on working days, excluding weekends and national holidays. In between of the testing, the sensor was left in the open air in the lab without any protection. Fig. 4 c) shows the characteristic output from the sensor for the first day of testing and the last day of testing. The output of the sensor is a short voltage pulse corresponding to the flush of water vapor on the sensor surface. Each of the peaks corresponds to one water vapor flush.

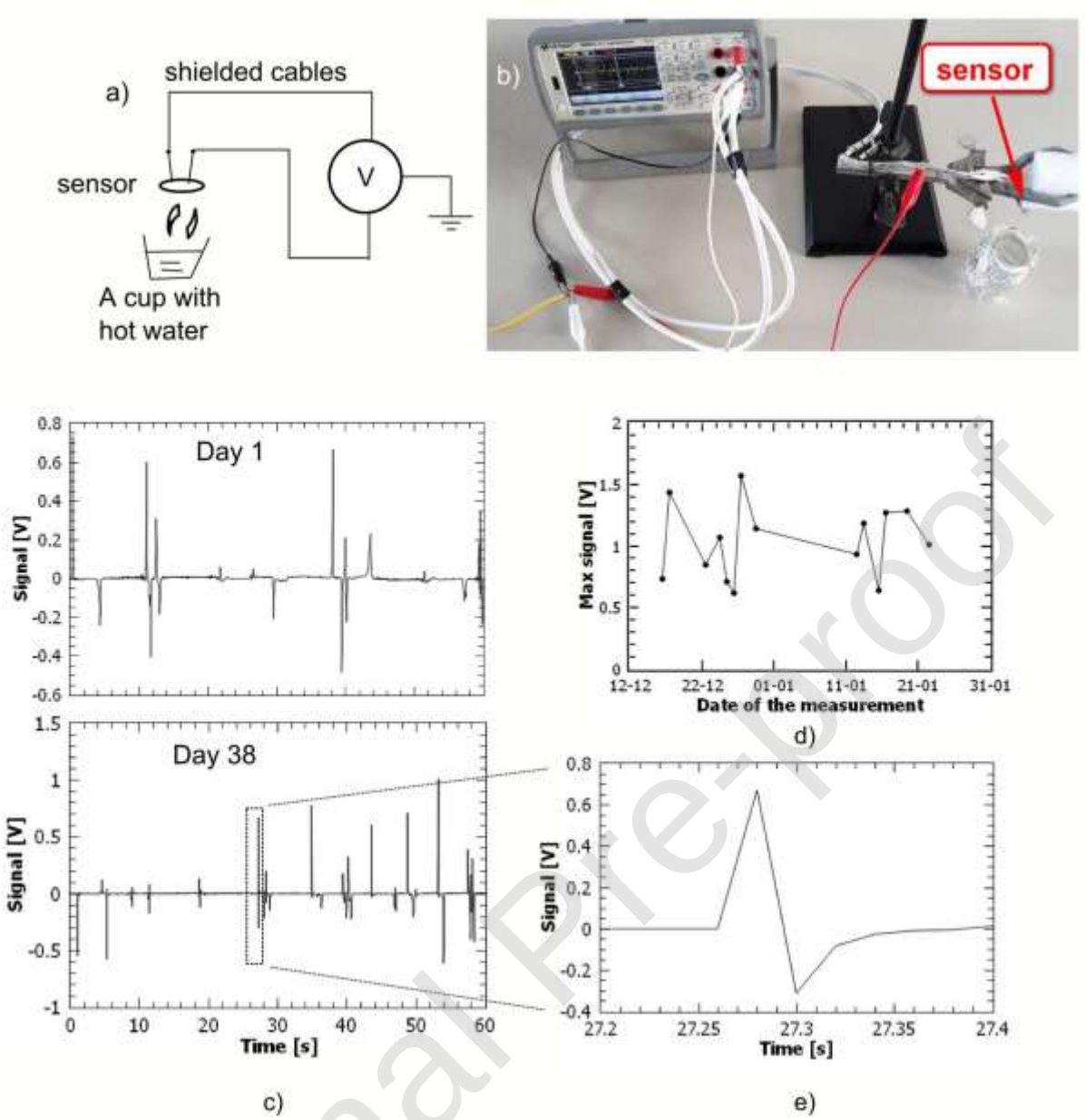

Fig. 4 a) Schematic of the experimental set-up. **b)** Photograph of the experimental set-up. **c)** Output signal from the sensor for Day 1 (the first day of testing) and Day 38 (the last day of testing). **d)** The absolute maximum value of the sensor signal for each day of the measurements **e)** A zoom into one of the voltage pulses during the sensor testing. The time resolution of the voltmeter was 20 ms.

The peaks are of various heights reflecting the fact that the amount of water vapor coming to the surface was not controllable. The sensor showed that it is capable of detecting water vapor flushes of various intensity, from very faint and short to much stronger. From Fig. 4 c) it is also visible that the polarity of the output of the sensor was unpredictable. This comes as a consequence of both electrodes of the sensor being made out of the same material. The electrodes are “deciding” among themselves which one will take the role of anode or cathode in every particular event of water vapor adsorption. The unpredictable polarity of output should not be a problem for modern electronics, since the signal could be easily rectified, so that only its absolute value is used. Fig. 4 e) shows a

zoom into one of the peaks. The total rise and fall time are typically less than 100 ms. The time resolution of the voltmeter was 20 ms. Fig. 4 d) shows the maximum absolute signal values for each of the days when testing was performed. It is obvious that the signal is not degrading, so it could be expected, that in this mode of operation, the sensor could be operational for a much longer period than it was here directly tested. Supplementary data contains numerical values for all test days [51]. The data presented in Fig. 4 c) is a 60 s excerpt from the measurements for Day 1 and Day 38.

In order to get a detailed recording of the transition process during water vapor detection, the sensor was connected to an oscilloscope (Tektronix TDS 3032B) over a pre-amp (SignalRecovery, Model 5113 Pre-amp, US) which serves to minimize the noise in the system by using the built in band pass filter, Fig. 5 a). Parameters for the oscilloscope have been: DC measurement, 20 MHz low pass filter, 1 MΩ input impedance. Parameters for the preamp have been: 250x gain, 1 to 30 Hz band pass filter (6 dB attenuation at the cut off frequency), 10 MΩ input impedance. The band pass filter was needed in order to avoid interference from external electromagnetic fields, mainly power network at 50 Hz. Fig. 5 b,c) shows the output from the sensor as recorded by oscilloscope during single water vapor flash. It is obvious that the rise time (i.e. the reaction of the sensor) was very fast, around 10 ms, while the relaxation of the system is relatively slower, around 50 ms. The reaction speed of the sensor makes it very fast in comparison to other breath detection sensors [15]. Mogera et al. show the fastest humidity sensor reported to date with the response time of only 8 ms [49]. Zhen et al. show the sensor reacting to water vapor in as low as 12.5 ms [50]. There is a relatively small number of sensors which have the reaction time below 100 ms [5]. It is important to notice that the relaxation here is happening in the form of damped oscillations. That is a consequence of the system sensor-cables-instrument actually forming an RLC circuit. In the starting moment the interdigitated capacitor of the sensor is charged. It discharges over the instrument and the cables which have a certain inductance which is producing damped oscillations, Fig. 5 c). The time resolution of the oscilloscope was 0.4 ms.

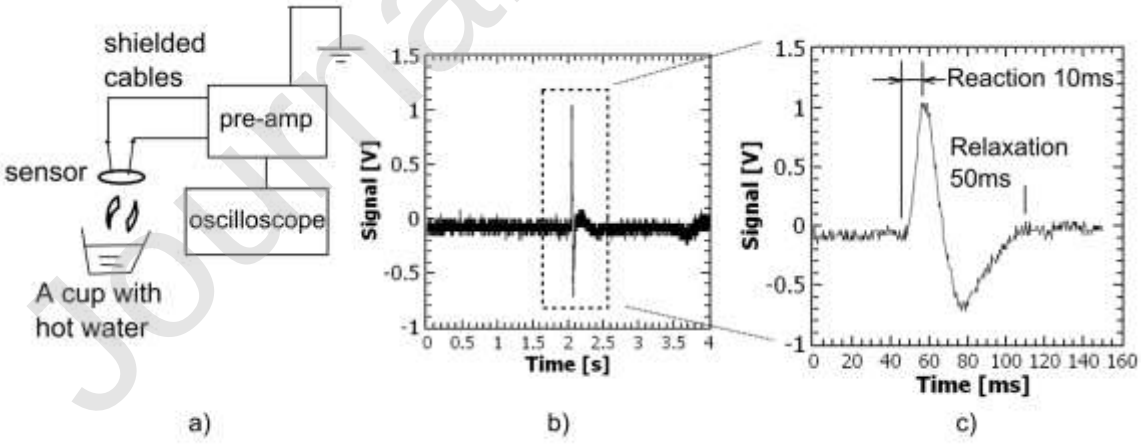

Fig. 5 Testing the transition process of the sensor response. **a)** Schematic of the set-up. **b)** Response of the sensor for a single event of the water vapor adsorption. **c)** A zoom into the transition process.

To test the longevity of the sensor it was kept in a closed glass bottle half filled with de-mineralized water at the temperature of 25°C, Fig. 6 a). In this way the sensor was constantly exposed to a high humidity level since the air was saturated with water vapor. One battery of the sensor was connected to 10 MΩ resistor so that the certain current was always flowing through the battery. The other battery was left with open ends so that the current was zero. The output voltage from the two batteries was measured once per day in the duration of 20 days. The result is given in Fig. 6 b). During the period of observation, the sensor`s battery which was connected to 10 MΩ resistor showed faster degradation than the battery which was left with the open ends, Fig. 6 b). The degradation is a consequence of consumption of the material out of which the electrodes are made. Given a practical usability as a breath detector, where, in the worst-case scenario, the sensor is exposed to high humidity level for 50% of the time, it could be expected that the sensor would survive at least two times longer compared with the total test time shown in Fig. 6. This should be satisfactory for any clinical application given that this kind of device needs to be replaced regularly due to the hygienic reasons. The energy produced by battery which was connected to the 10 MΩ resistor was 0.11 μWh (0.4 mJ) which means that the surface energy density from the single sensor battery was 33.8 mJ cm^{-2}.

With the same set-up, the temperature of water was slowly increased from 25°C to 80°C. The signal change was within 2%. Separately, the sensor was tested in open air by exposing it to a direct blow of hot air from a fan heater. No signal was observed.

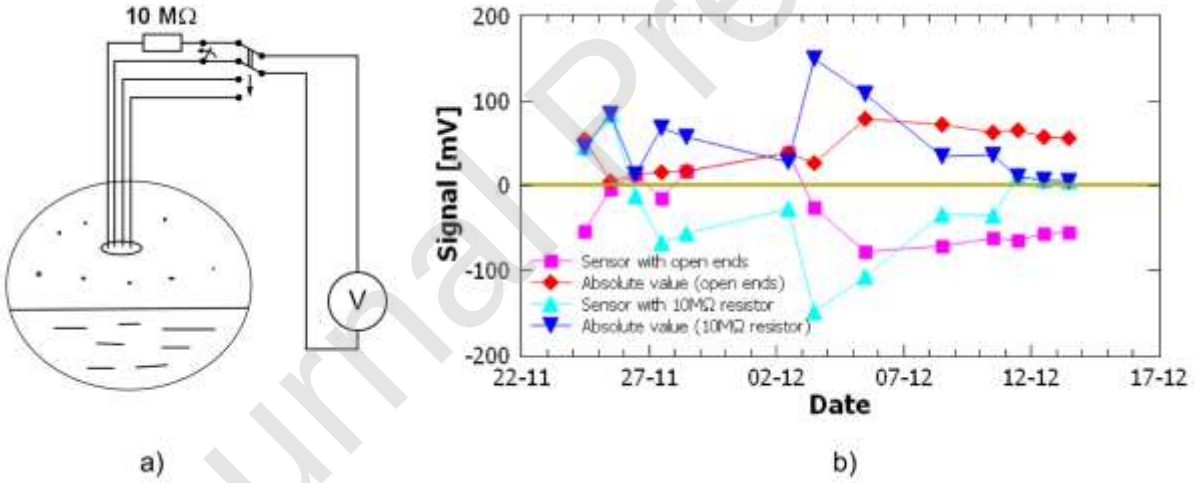

Fig. 6 Longevity test of the breath humidity sensor. **a)** Schematic of the set-up. The batteries of the sensor have been connected to the voltmeter once per day. **b)** Data collected after 20 days of measurements. Since the polarity of the sensor output was variable from day to day, the absolute values are also plotted.

3.2 Electrochemistry of the device

This is a completely novel concept of the sensor or battery device, so the current understanding of some of the aspects of the device functionality is limited. The closest match to this is the class of metal-air batteries [44-46]. The aluminum-air battery is again the closest to the

operation of this device since the electrodes are 99% aluminum. The electrochemical reactions taking place at the electrodes in the presence of water and air could be described as follows:

Anode: $Al(s) + 3OH^-(aq) \rightarrow Al(OH)_3(s) + 3e^-$ (1)

Cathode: $O_2(g) + 2H_2O(l) + 4e^- \rightarrow 4OH^-(aq)$ (2)

Overall: $4Al(s) + 3O_2(g) + 6H_2O(l) \rightarrow 4Al(OH)_3(s)$ (3) [46].

It is evident that the cathode material does not play a crucial role herein, since it does not appear in (2). For this reason, it is possible to have an operational aluminum-air battery even with both electrodes made out of aluminum i.e. the same material. This structure will bring an uncertainty in the polarity which electrodes are making. In one situation, one electrode could be the anode, and in the next situation the same electrode could play the role of the cathode. This causes the changeable polarity of the output voltage of the described device, which was observed in the experiments.

The theoretical value of the voltage produced in electrochemical process described by (1-3) is 2.7 V [52]. In practical measurements lower values are obtained [53]. The voltage depends on the structure of the electrodes and the type of the electrolyte. In the experiment shown in Fig. 6 the voltage obtained was around 100 mV. This is mainly a consequence of the parasitic resistor which is formed by the DM water layer connecting the electrodes. Fig. 7 a) gives an equivalent schematic of the sensor and voltmeter in this case. In Fig. 7 a), E is the electromotive force produced by electrodes, Cp is the parasitic capacitance as formed by interdigitated capacitor of the sensor, Rp is the parasitic resistor and Rg is the input resistance of the voltmeter. For DC current, measured voltage will depend on the parasitic resistor according to the equation (Ohm`s law): U = E Rg / (Rg+Rp), where U is the measured voltage. If E = 2.7 V, U = 100 mV and Rg = 10 MΩ, calculated Rp = 260 MΩ. Parasitic capacitor Cp (20pF as measured by RLC meter at 10kHz in dry air) will bypass Rp and enable higher measured voltage for pulsed or changeable signal what is seen in Fig. 4. Another point is that the electrodes are made out of the same material which can make them work against each other, i.e. produce the same polarity and effectively reduce the output voltage.

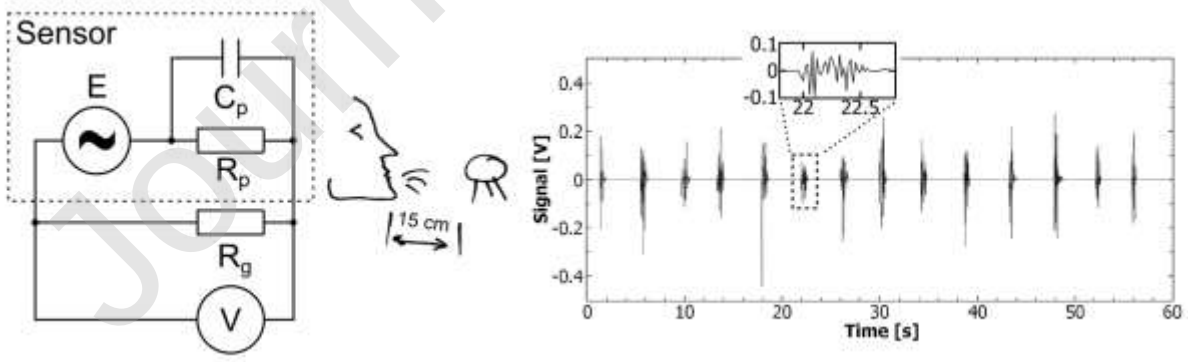

a) **b)** **c)**

Fig. 7 a) The equivalent schematic of the sensor connected to the voltmeter. E is the electromotive force generated by electrodes, Cp is the parasitic capacitor, Rp is the parasitic resistor and Rg is the input resistance of the voltmeter. **b)** The illustration of the experiment. **c)** Response of the sensor to the direct breath blow. The sensor was in the open air. It was blown by the human breath from the distance of around 15 cm. The diagram represents the last 60 s of the measurement. The numerical data of the full measurement and the

video describing the experiment are available in supplementary data [54].

The changes in O_2 levels can also influence the output of the sensor. Influence of O_2 level is present in (2). The experiment with a cup of hot water is happening at 21% O_2 concentration in air. The experiment with human breath should have 16% of O_2 in the exhaled air. This can make a difference in the sensor output for the same amount of humidity. Since the sensor is not intended for relative humidity measurement, this quantitative difference would make little effect on the detection of human breath. The sensor produced no signal when tested by direct blow of dry O_2 in the open air.

The condensation of the water vapor on the surface of electrodes is necessary for the generation of the sensor output voltage. The water vapor serves two functions. One is in the process of generating charge in the interaction with aluminum and the other is to make a conductive path between the sensor electrodes in order to close the electrical circuit. For this reason the water vapor needs to form a continuous film on the sensor`s surface.

According to (3) the aluminum hydroxide should remain on the surface of the sensor as an end-product. In this work, this was considered as a nuisance which can deteriorate the performance of the sensor. For this reason longevity tests have been performed. In the experiment presented in Fig. 4 there was no visible deterioration of the sensor performance during the test period. In the experiment shown in Fig. 6 the deterioration of the performance was due to the consumption of the material out of which the electrodes are made. The aluminum hydroxide can play a role in the diminishing signal seen in Fig. 6.

3.3 Breath detection test

The response of the sensor to the direct breath blow is shown in Fig. 7 b, c). The sensor was placed in open air and connected to the voltmeter. The parameters of the voltmeter were: range:10 V, time resolution 20 ms, input resistivity 10 MΩ. The sensor was blown by direct breath from a distance of around 15 cm. The duration of every blow was very short, around 0.5 s. The waiting time was around 5 s. The humidity, together with oxygen coming to the sensor surface produced the signal. The signal was changing the polarity very fast but it was also reacting very fast to the breath blow. The noise was well below the signal, estimated at 0.5 mV. Every event of the breath blow was clearly separated. The diagram presented in Fig. 7 c) presents the last 60 s of the measurement. The full numerical data is given in supplementary data [54] together with the short video describing the experimental procedure.

In order to show the usefulness of the proposed sensor, a test with the human respiration was made. The breathing mask, normally used for oxygen, was used by a volunteer. The sensor was mounted to the end of the tube which was at the other end attached to the breathing mask, so that the air could have an unobstructed flow over the active sensor`s surface, Fig. 8 a). The output from the sensor for various breathing rates is given in Fig. 8 b). The sensor was capable of following the complete breathing cycle, comprised of inhaling of the fresh air and exhaling of the moisturized air. The rise of the signal follows the water vapor accumulation on the sensor`s surface during exhaling. The fall of the signal follows the drying of the sensor`s surface by the fresh air which was inhaled.

The rate of the sensor response was high enough so that the sensor was able to follow the fastest breathing pace in this testing, up to 25 cycles per minute (cpm). Normal breathing was measured as 17 cpm and slower breathing had 13 cpm, Fig. 8 b). The response of the sensor in this case was different from that depicted in Fig. 4, 5 and 7 b, c) because of different experimental conditions. In Fig. 8 the sensor was closed in the tube thus having more stable humidity and oxygen levels, while in Fig. 4, 5 and 7 b, c) it was in the open air thus having more random fluctuations of water vapor and oxygen. For this reason, in Fig. 4, 5 and 7 b, c) the response was spike-like while in Fig. 8 it was continuous. In Fig. 8 relatively good repeatability of the sensor signal was observed. The polarity change was not observed during this breath humidity measurement. In general, polarity change does happen during respiration monitoring. The signal could be easily rectified by modern electronics and the absolute value should be used.

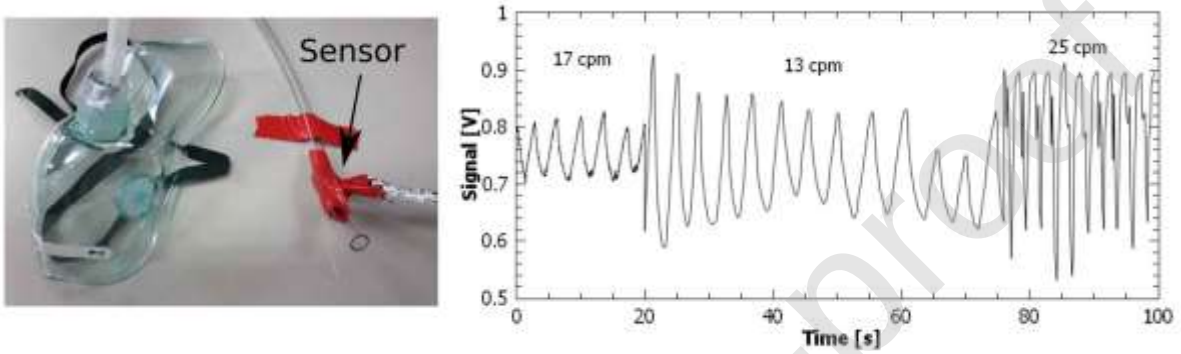

Fig. 8 a) The breathing mask with the sensor attached at the end of the tube. **b)** The sensor output during breathing with various paces.

Response of the sensor to the lower concentrations of water vapor, lower from what is achievable by direct water vapor flush or human breath, was too noisy, so that the same approach cannot be applied for RH measurement. The possible applicability of the sensor, so far demonstrated, is for breath humidity detection.

4. Conclusions

The sensor presented here is capable of very fast reaction to 100% RH which makes it suitable for breath humidity detection. The key advantage of the sensor is that it is a self-powered device generating electricity in the process of water vapor detection itself. Therefore, there is no need for any external power supply or energy harvesting device. The energy is practically harvested from the interaction of aluminum and water. There are only few solutions like this published to date [38-44] but with different materials and more complicated fabrication. The sensor is very fast with response time down to 10 ms. Damped oscillations have been observed during the relaxation process, and they are related to the construction of the sensor and the measurement system. The absolute value of the signal was up to 1.5 V, which is easily measurable with standard instruments or custom electronics. The signal was high above the noise in the measurement system, but special care needs to be taken to shield and ground the transmission cables and instruments. Longevity of the sensor was tested, and the sensor proved to be functional in the period of more than one

month. The sensor used for breath detection should be regularly replaced due to hygienic reasons. In this sense the anticipated lifetime should be sufficient for clinical use. Practical application for breath monitoring was shown for different breathing rates, normal, faster and slower than normal. The sensor was capable of resolving various speeds of breathing. The sensor is relatively small. A single battery active area is only 1.58 mm x 0.74 mm or 1.17 mm^2. Therefore, it is suitable for use in portable or wearable applications. It also has a potential to be realized on flexible substrates, since Al 1%Si thin film is flexible and the Si substrate presented in this work has no influence on the interaction between Al and water vapor. The construction of the sensor is relatively simple and easy to fabricate with modern planar technology. The materials used in the sensor construction are not toxic and not volatile, which is beneficial for medical applications.

Apart from water vapor, it is reasonable to expect that also some other chemicals or gases could be detected with this kind of device, first of all, electrolytes used in metal-air batteries. The other metals can be tested as active sensing materials. The metal-air batteries can be realized using other metals like Fe, Mg or Li [44]. One direction of further development is testing use of various metals but also various geometries of the sensor electrodes. The influence of Si, or any other impurities present in the active layer of Al 1%Si on power generation has to be further examined. An additional key topic of further work will be full understanding of the electrochemistry involved in the operation of this device, especially the variable polarity that happens in the process of humidity sensing. The range of the sensor applicability is, so far, only for measurement of the high RH values as produced by direct water vapor flush or by human breath. Further work will be focused on enabling the sensor to perform accurate measurements at lower RH levels.

CRediT author statement

Marko V Bošković: Conceptualization, Validation, Investigation, Writing - Review & Editing **Milija Sarajlić:** Conceptualization, Validation, Investigation, Writing - Original Draft, Supervision **Miloš Frantlović:** Investigation, Writing - Review & Editing **Milče M Smiljanić:** Investigation, Writing - Review & Editing **Danijela V Randelović:** Investigation, Writing - Review & Editing **Katarina Cvetanović Zobenica:** Investigation, Writing - Review & Editing **Dana Vasiljević Radović:** Investigation, Writing - Review & Editing, Project administration, Funding acquisition.

Declaration of interests

The authors declare that they have no known competing financial interests or personal relationships that could have appeared to influence the work reported in this paper.

Declaration of Competing Interest

The authors declare that there are no conflicts of interest.

Acknowledgements

This work was financially supported by the Ministry of Education, Science and Technological Development of the Republic of Serbia (Grant No. 451-03-68/2020-14/200026). The authors would like to thank Prof. Dr. Biljana Šljukić Paunković, Faculty of Physical Chemistry, University of Belgrade, for her helpful advice on electrochemical issues examined in this paper.

References

[1] Ehsanul Kabir, Nadeem Raza, Vanish Kumar, Jagpreet Singh, Yiu Fai Tsang, Dong Kwon Lim, Jan Edward Szulejko, Ki-Hyun Kim, Recent Advances in Nanomaterial-Based Human Breath Analytical Technology for Clinical Diagnosis and the Way Forward, *Chem* **5** 12 (2019) 3020-3057 doi: 10.1016/j.chempr.2019.08.004.

[2] Alessio Ceccarini, Fabio Di Francesco, Roger Fuoco, Silvia Ghimenti, Massimo Onor, Sara Tabucchi, Maria Giovanna Trivella, Breath Analysis: Analytical Methodologies and Clinical Applications, Chapter 23, doi: 10.1002/9781118271858.ch23 in *Analytical Techniques for Clinical Chemistry: Methods and Applications* Editor(s): Sergio Caroli Gyula Záray, First published: 22 June 2012, Print ISBN:9780470445273 |Online ISBN:9781118271858 |DOI:10.1002/9781118271858, Copyright © 2012 John Wiley & Sons, Inc.

[3] Jonathan D Beauchamp, Joachim D Pleil, Breath: An Often Overlooked Medium in Biomarker Discovery, Chapter 5, doi: 10.1002/9783527680658.ch5 in *Biomarker Validation* Editor(s): Harald Seitz Sarah Schumacher, First published: 27 February 2015, Print ISBN:9783527337194 |Online ISBN:9783527680658 |DOI:10.1002/9783527680658, Copyright © 2015 Wiley-VCH Verlag GmbH & Co. KgaA

[4] Jianxun Dai, Hongran Zhao, Xiuzhu Lin, Sen Liu, Teng Fei, Tong Zhang, Design strategy for ultrafast-response humidity sensors based on gel polymer electrolytes and application for detecting respiration *Sensors & Actuators: B. Chemical* **304** 127270 (2020) doi: 10.1016/j.snb.2019.127270.

[5] Jianxun Dai, Hongran Zhao, Xiuzhu Lin, Sen Liu, Yunshi Liu, Xiupeng Liu, Teng Fei, and Tong Zhang, Ultrafast Response Polyelectrolyte Humidity Sensor for Respiration Monitoring, *ACS Appl. Mater. Interfaces* **11** 6483−6490 (2019) DOI: 10.1021/acsami.8b18904.

[6] Biqiang Jiang, Zhixuan Bi, Zhen Hao, Qingchen Yuan, Dingyi Feng, Kaiming Zhou, Lin Zhang, Xuetao Gan, Jianlin Zhao, Graphene oxide-deposited tilted fiber grating for ultrafast humidity sensing and human breath monitoring, *Sensors & Actuators: B. Chemical* **293** 336–341 (2019) doi: 10.1016/j.snb.2019.05.024.

[7] Bolun Li, Qi Tian, Hongxin Su, Xingwei Wang, Tianen Wang, Dongzhi Zhang, High sensitivity portable capacitive humidity sensor based on In2O3 nanocubes-decorated GO nanosheets and its wearable application in respiration detection *Sensors & Actuators: B. Chemical* **299** 126973 (2019) doi: 10.1016/j.snb.2019.126973.

[8] Bobo Du, Dexing Yang, Xiaoyang She, Yuan Yuan, Dong Mao, Yajun Jiang, Fanfan Lu, MoS2-based all-fiber humidity sensor for monitoring human breath with fast response and recovery *Sensors and Actuators B* **251** 180–184 (2017) doi: 10.1016/j.snb.2017.04.193.

[9] Jin Zhou, Xin Xiao, Xue-Feng Cheng, Bi-Jun Gao, Jing-Hui He, Qing-Feng Xu, Hua Li, Na-Jun Li, Dong-Yun Chen, Jian-Mei Lu, Surface modification of polysquaraines to sense humidity within a second for breath monitoring *Sensors & Actuators: B. Chemical* **271** 137–146 (2018) doi.org/10.1016/j.snb.2018.05.085.

[10] Hamid Farahani, Rahman Wagiran and Mohd Nizar Hamidon, Humidity Sensors Principle, Mechanism, and Fabrication Technologies: A Comprehensive Review *Sensors* **14** 7881-7939 (2014) doi:10.3390/s140507881.

[11] T.A. Blank, L.P. Eksperiandova, K.N. Belikov, Recent trends of ceramic humidity sensors development: A review *Sensors and Actuators B* **228** 416–442 (2016) doi: 10.1016/j.snb.2016.01.015.

[12] P T Moseley, Solid state gas sensors *Meas. Sci. Technol.* **8** 223 (1997) doi: 10.1088/0957-0233/8/3/003.

[13] WATER VAPOUR SORPTION AND HUMIDITY – A SURVEY ON MEASURING METHODS AND STANDARDS, Erich Robens, Katrin Rübner, Peter Klobes and Devrim Balköse, Chapter 1 in: *Humidity Sensors* Editor: Christopher T. Okada © 2011 Nova Science Publishers, Inc. ISBN 978-1-61209-246-1.

[14] Hengchang Bi, Kuibo Yin, Xiao Xie, Jing Ji, Shu Wan, Litao Sun, Mauricio Terrones and Mildred S. Dresselhaus, Ultrahigh humidity sensitivity of graphene oxide *SCIENTIFIC REPORTS* **3** 2714 (2013) doi: 10.1038/srep02714.

[15] Stefano Borini, Richard White, Di Wei, Michael Astley, Samiul Haque, Elisabetta Spigone, Nadine Harris, Jani Kivioja, and Tapani Ryhanen, Ultrafast Graphene Oxide Humidity Sensors, *ACS Nano* 7 **12** pp. 11166-11173 (2013) doi: 10.1021/nn404889b.

[16] Abdul Rahman, Mohd Syaifudin, Mukhopadhyay, Subhas Chandra, Yu, Pak Lam, *Novel Planar Interdigital Sensors* in *Novel Sensors for Food Inspection: Modelling, Fabrication and Experimentation*, Springer International Publishing, (2014) ISBN 978-3-319-04273-2.

[17] Tarikul Islam, A.T. Nimal, Upendra Mittal, M.U. Sharma, A micro interdigitated thin film metal oxide capacitive sensor for measuring moisture in the range of 175–625 ppm *Sensors and Actuators B* **221** (2015) 357–364 doi: 10.1016/j.snb.2015.06.101.

[18] Jinguang Cai, Chao Lv, Eiji Aoyagi, Sayaka Ogawa and Akira Watanabe, Laser Direct Writing of a High-Performance All-Graphene Humidity Sensor Working in a Novel Sensing Mode for Portable Electronics *ACS Appl. Mater. Interfaces* **10** 23987−23996 (2018) DOI: 10.1021/acsami.8b07373.

[19] María Cuartero and Gastón A. Crespo, All-solid-state potentiometric sensors: A new wave for in situ aquatic research *Current Opinion in Electrochemistry* **10** 98–106 (2018) doi: 10.1016/j.coelec.2018.04.004.

[20] Chengmei Jiang, Yao Yao, Yalu Cai, Jianfeng Ping, All-solid-state potentiometric sensor using single-walled carbon nanohorns as transducer *Sensors & Actuators: B. Chemical* **283** (2019) 284–289 doi: 10.1016/j.snb.2018.12.040.

[21] T.F.A. Sousa, C.G. Amorim, M.C.B.S.M. Montenegro, A.N. Araújo, Cyclodextrin based potentiometric sensor for determination of ibuprofen in pharmaceuticals and waters *Sensors and Actuators B* **176** pp. 660–666 (2013) doi: 10.1016/j.snb.2012.09.016.

[22] Alexander Volkov, Elena Gorbova, Aleksey Vylkov, Dmitry Medvedev, Anatoly Demin, Panagiotis Tsiakaras, Design and applications of potentiometric sensors based on proton-conducting ceramic materials. A brief review *Sensors and Actuators B* **244** 1004–1015 (2017) doi: 10.1016/j.snb.2017.01.097.

[23] Suvra Prakash Mondal, Prabir K. Dutta, G.W. Hunter, B.J. Ward, D. Laskowski, R.A. Dweik, Development of high sensitivity potentiometric NOx sensor and its application to breath analysis *Sensors and Actuators B* **158** 292–298 (2011) doi:10.1016/j.snb.2011.05.063.

[24] M.S. Cosio, M. Scampicchioy, S. Benedetti, Electronic Noses and Tongues, pp. 219-247, Chapter 8 in *Chemical Analysis of Food: Techniques and Applications*, Editor: Yolanda Picó, Copyright 2012 Elsevier Inc. DOI: 10.1016/B978-0-12-384862-8.00008-X.

[25] Dong-Hoon Choi, Yi Li, Garry R. Cutting, Peter C. Searson, A wearable potentiometric sensor with integrated salt bridge for sweat chloride measurement *Sensors and Actuators B* **250** 673–678 (2017), doi: 10.1016/j.snb.2017.04.129

[26] Toshikatsu Sata, Possibility for potentiometric humidity sensor of composite membranes prepared from anion-exchange membranes and conducting polymer *Sensors and Actuators B: Chemical* **23** 1 (1995) pp. 63-69. doi: 10.1016/0925-4005(94)01524-L.

[27] M.A Hassen, A.G Clarke M.A Swetnam, R.V Kumar, D.J Fray, High temperature humidity monitoring using doped strontium cerate sensors *Sensors and Actuators B: Chemical* **69** 138-143 (2000) doi: 10.1016/S0925-4005(00)00530-X.

[28] Chao-Nan Xu, Kazuhide Miyazaki, Tadahiko Watanabe, Humidity sensors using manganese oxides *Sensors and Actuators B: Chemical* **46** 87-96 (1998) doi: 10.1016/S0925-4005(97)00330-4.

[29] Jing Zhang, Gaopeng Jiang, Timothy Cumberland, Pan Xu, Yalin Wu, Stephen Delaat, Aiping Yu, Zhongwei Chen, A highly sensitive breathable fuel cell gas sensor with nanocomposite solid electrolyte, *InfoMat* **1** 234–241 (2019) doi: 10.1002/inf2.12017.

[30] Mohammadreza Zamanzad Ghavidel, Mohammad R. Rahman, E. Bradley Easton, Fuel cell-based breath alcohol sensors utilizing Pt-alloy electrocatalysts, *Sensors & Actuators: B. Chemical* **273** 574–584 (2018) doi: 10.1016/j.snb.2018.06.078.

[31] Jie Yang, Sasan Ghobadian, Payton J. Goodrich, Reza Montazami and Nastaran Hashemi, Miniaturized biological and electrochemical fuel cells: challenges and applications *Phys. Chem. Chem. Phys.* **15** 14147 (2013) DOI: 10.1039/c3cp50804h.

[32] Venkateswaran Vivekananthan, Nagamalleswara Rao Alluri, Yuvasree Purusothaman, Arunkumar Chandrasekhar, Sophia Selvarajan and Sang-Jae Kim, Biocompatible Collagen Nanofibrils: An Approach for Sustainable Energy Harvesting and Battery-Free Humidity Sensor Applications *ACS Appl. Mater. Interfaces* **10**, 18650−18656 (2018) DOI: 10.1021/acsami.8b02915.

[33] Yan Zhang, Mengying Xie, Vana Adamaki, Hamideh Khanbareh and Chris R. Bowen, Control of electro-chemical processes using energy harvesting materials and devices *Chem. Soc. Rev.* **46** 7757 (2017) DOI: 10.1039/c7cs00387k.

[34] Yuanjie Su, Guangzhong Xie, Si Wang, Huiling Tai, Qiuping Zhang, Hongfei Du, Hulin Zhang, Xiaosong Du, Yadong Jiang, Novel high-performance self-powered humidity detection enabled by triboelectric effect *Sensors and Actuators B* **251** 144–152 (2017) doi: 10.1016/j.snb.2017.04.039.

[35] He Zhang, Jiwei Zhang, Zhiwei Hu, Liwei Quan, Lin Shi, Jinkai Chen, Weipeng Xuan, Zhicheng Zhang, Shurong Dong, Jikui Luo, Waist-wearable wireless respiration sensor based on triboelectric effect, *Nano Energy* 59 75–83 (2019) doi: 10.1016/j.nanoen.2019.01.063.

[36] Zhen Wen, Jun Chen, Min-Hsin Yeh, Hengyu Guo, Zhaoling Li, Xing Fan, Tiejun Zhang, Liping Zhu, Zhong Lin Wang, Blow-driven triboelectric nanogenerator as an active alcohol breath analyzer *Nano Energy* **16** 38–46 (2015) doi: 10.1016/j.nanoen.2015.06.006.

[37] Siwen Cui, Youbin Zheng, Tingting Zhang, Daoai Wang, Feng Zhou, Weimin Liu, Self-powered ammonia nanosensor based on the integration of the gas sensor and triboelectric nanogenerator *Nano Energy* **49** 31–39 (2018) doi: 10.1016/j.nanoen.2018.04.033.

[38] Daozhi Shen, Ming Xiao, Guisheng Zou, Lei Liu, Walter W. Duley, and Y. Norman Zhou, Self-Powered Wearable Electronics Based on Moisture Enabled Electricity Generation *Adv. Mater.* **30** 1705925 (2018) DOI: 10.1002/adma.201705925.

[39] Daozhi Shen, Ming Xiao, Yu Xiao, Guisheng Zou, Lifang Hu, Bo Zhao, Lei Liu, Walter W. Duley, and Y. Norman Zhou, Self-Powered, Rapid-Response, and Highly Flexible Humidity Sensors Based on Moisture-Dependent Voltage Generation *ACS Appl. Mater. Interfaces* **11** 14249−14255 (2019) DOI: 10.1021/acsami.9b01523.

[40] Yu Xiao, Daozhi Shen, Guisheng Zou, Aiping Wu, Lei Liu, Walter W Duley and Y Norman Zhou, Self-powered, flexible and remote-controlled breath monitor based on TiO2 nanowire networks *Nanotechnology* **30** 325503 (2019) doi: 10.1088/1361-6528/ab1b93.

[41] Fei Zhao, Huhu Cheng, Zhipan Zhang, Lan Jiang, and Liangti Qu, Direct Power Generation from a Graphene Oxide Film under Moisture *Adv. Mater.* **27** 4351–4357 (2015) DOI: 10.1002/adma.201501867.

[42] Fei Zhao, Yuan Liang, Huhu Cheng, Lan Jiang and Liangti Qu, Highly efficient moisture-enabled electricity generation from graphene oxide frameworks *Energy Environ. Sci.* **9** 912 (2016) DOI: 10.1039/c5ee03701h.

[43] Kang Liu, Peihua Yang, Song Li, Jia Li, Tianpeng Ding, Guobin Xue, Qian Chen, Guang Feng, and Jun Zhou, Induced Potential in Porous Carbon Films through Water Vapor Absorption *Angew. Chem. Int. Ed.* **55** 8003–8007 (2016) DOI: 10.1002/anie.201602708.

[44] Xiaomeng Liu, Hongyan Gao, Joy E. Ward, Xiaorong Liu, Bing Yin, Tianda Fu, Jianhan Chen, Derek R. Lovley, Jun Yao, Power generation from ambient humidity using protein nanowires *Nature* **578** p550–554 (2020) doi:10.1038/s41586-020-2010-9.

[45] Chunlian Wang, Yongchao Yu, Jiajia Niu, Yaxuan Liu, Denzel Bridges, Xianqiang Liu, Joshi Pooran, Yuefei Zhang and Anming Hu, Recent Progress of Metal–Air Batteries—A Mini Review *Appl. Sci.* **9** 2787 (2019) doi: 10.3390/app9142787.

[46] Modesto Tamez and Julie H. Yu, Aluminum–Air Battery *Journal of Chemical Education* **84** 12 (2007) doi: 10.1021/ed084p1936A.

[47] Anton Van der Ven, Brian Puchala, Takeshi Nagase, Ti- and Zr-based metal-air batteries *Journal of Power Sources* **242** 400-404 (2013) doi: 10.1016/j.jpowsour.2013.05.074.

[48] Greg M. Swain, *Solid Electrode Materials: Pretreatment and Activation* in *Handbook of Electrochemistry* (2007) Elsevier B.V. Edited by C.G. Zoski, ISBN: 9780444519580.

[49] Umesha Mogera, Abhay A. Sagade, Subi J. George & Giridhar U. Kulkarni, Ultrafast response humidity sensor using supramolecular nanofibre and its application in monitoring breath humidity and flow *SCIENTIFIC REPORTS* **4** 4103 (2014) DOI: 10.1038/srep04103.

[50] Zhen Zhen, Zechen Li, Xuanliang Zhao, Yujia Zhong, Li Zhang, Qiao Chen, Tingting Yang, and Hongwei Zhu, Formation of Uniform Water Microdroplets on Wrinkled Graphene for Ultrafast Humidity Sensing *Small* **14** 1703848 (2018) DOI: 10.1002/smll.201703848.

[51] Milija Sarajlic et al. *Mendeley Data* **V1** (2020) doi: 10.17632/g23fv2xbbf.1

[52] Bratsch, S. G., Standard Electrode Potentials and Temperature Coefficients in Water at 298.15 K, *J. Phys. Chem. Ref. Data* **18** 1−21 (1989) doi: 10.1063/1.555839

[53] Leanne D. Chen, Jens K. Nørskov, and Alan C. Luntz, Al−Air Batteries: Fundamental Thermodynamic Limitations from First-Principles Theory *J. Phys. Chem. Lett.* **6** 175−179 (2015) doi: 10.1021/jz502422v

[54] Milija Sarajlic et al., Supplementary data 2 *Mendeley Data* **V1** (2020) doi: 10.17632/hny6rfv9sm.1

Marko V. Bosković holds MSc in physical chemistry, from the Faculty of Physical Chemistry, University of Belgrade, Serbia. He is employed as a Junior Researcher at the Department of Microelectronic Technologies, Institute of Chemistry, Technology, and Metallurgy, University of Belgrade. His fields of interest are Electrochemical Sensors and Self-powered Sensors.

Milija Sarajlić holds PhD in Applied Physics from the Physics Faculty, University of Belgrade, Serbia. He is employed at ICTM CMT, Belgrade, Serbia as Associate Research Professor. He has spent four years as a postdoc at DESY research center in Hamburg, Germany. His fields of interest are: Chemical Sensors, Thin Film Sensors and Semiconductor Technology.

Miloš Frantlović received his Dipl. Ing., Mag. Sci. and Ph. D. degrees from the School of Electrical Engineering, University of Belgrade, Serbia. Currently, he is Senior Research Associate at the Center of Microelectronic Technologies (CMT), Institute of Chemistry, Technology and Metallurgy (ICTM), University of Belgrade. His main area of expertise is the research and development of electronic instrumentation based on MEMS sensors. He is also involved in the research of chemical, biochemical and other MEMS/NEMS sensors.

Milče M. Smiljanić received her Dipl.ing, Mag. sci. and Ph.D. degrees in electrical engineering from the School of Electrical Engineering, University of Belgrade. Currently, she is an senior research associate at the Institute of Chemistry, Technology and Metallurgy, Center for Microelectronic Technologies (ICTM-CMT). Her research interests are micromachining of silicon and Pyrex glass for various sensors and actuators, piezoresistive pressure sensors and microcantilevers, Au based microcantilevers for magnetic field measurement, silicon photodiodes, microreactors.

Dr Danijela V. Randjelović, Full Research Professor, is with ICTM - CMT, University of Belgrade, since 1996. She received her Dipl.-Ing., Magister and Doctor of Science degrees in electrical engineering from the Faculty of Electrical Engineering, University of Belgrade, Serbia. She has been working in different fields of research with the main focuses on multipurpose thermopile-based MEMS sensors (vacuum, flow and gas sensors, thermal converters), Microbial Fuel Cells and AFM characterization of materials, MEMS/NEMS components, bacteria and nanoemulsions for drug delivery. She was leading subprojects and project tasks within several international and national projects. She is IEEE member, evaluator of
EU-funded projects and results of her scientific research were published in more than 100 papers in peer-reviewed journals and conference proceedings.

Katarina Cvetanović Zobenica was born in Belgrade, Serbia. She earned her Dipl. Phys.-Chem. and M.Sc. degrees in physical chemistry from the Faculty of physical chemistry, University of Belgrade. She is a research assistant at the Institute of Chemistry, Technology and Metallurgy, Center for Microelectronic Technologies. Her fields of interest are microsystem technologies (including

oxidation and photolithography), graphene membranes and dye-sensitized solar cells, with natural pigment - hypericin.

Dr Dana Vasiljević Radović is full research professor and director with the Center of Microelectronic Technologies, Institute of Chemistry, Technology and Metallurgy, University of Belgrade. She obtained her PhD degree in Materials Science from the University of Belgrade in 1997. Her interests include research and development of micro/nanosystems (MEMS and NEMS) based sensors, detectors and actuators. She has published more than 140 scientific papers, among these 75 papers published in peer-reviewed international scientific journals. She leads more R&D projects in the field of micro/nano-electro-mechanical-systems (MEMS/NEMS) as well as EU funded projects.